Electron Heating in a Low-Mach number Perpendicular Shocks I. Heating Mechanism

The Astrophysical Journal, 851:134 (23pp), 2017 December 20 https://doi.org/10.3847/1538-4357/aa9b82

Electron Heating in Low-Mach-number Perpendicular Shocks. I. Heating Mechanism

Xinyi Guo[1], Lorenzo Sironi[2], and Ramesh Narayan[1]
[1] Harvard-Smithsonian Center for Astrophysics, 60 Garden Street, Cambridge, MA 02138, USA; xinyi.guo@cfa.harvard.edu, rnarayan@cfa.harvard.edu
[2] Department of Astronomy, Columbia University, 550 W 120th St, New York, NY 10027, USA; lsironi@astro.columbia.edu
Received 2017 October 19; revised 2017 November 7; accepted 2017 November 15; published 2017 December 20

Abstract

Recent X-ray observations of merger shocks in galaxy clusters have shown that the postshock plasma has two temperatures, with the protons hotter than the electrons. By means of two-dimensional particle-in-cell simulations, we study the physics of electron irreversible heating in low-Mach-number perpendicular shocks, for a representative case with sonic Mach number of 3 and plasma beta of 16. We find that two basic ingredients are needed for electron entropy production: (1) an electron temperature anisotropy, induced by field amplification

Sandeep Kumar

CHEA Journal Club, UNIST [2018-03-22]

Contents

Introduction

- Galaxy Clusters grow by merging of the sub-clusters.
- A large fraction of the kinetic energy of in-falling sub-clusters is dissipated at low mach number shocks ($M_s \leq 5$) . (Sarazin 2002; Ryu et al. 2003; Bruggen et al. 2012)
- These shocks are routinely observed in X-ray and radio bands.
- However, these observational diagnostics are based on radiation emitted by electrons, the proton properties (especially their temperature) are basically unconstrained.
- Equal temperature of electrons and protons unlikely to hold in the vicinity of merger shocks. The bulk kinetic energy of protons is larger than for electrons. Therefore a comparable ratio should persist between the post-shock temperatures of the two species.
- Moreover, It has long been thought that collisionless shocks can lead to a two-temperature structure at the outskirts of galaxy clusters.

The Physics of electron heating

The work done on an anisotropic gas

$$dW = -P_{\perp} dV_{\perp} - P_{\parallel} dV_{\parallel}$$

The work done per particle $dw = \frac{dW}{N}$

$$dw = k_B T_{\perp} d\ln B + k_B T_{\parallel} d\ln\left(\frac{n}{B}\right)$$

change of internal energy per particle

$$du_{\perp} = dw_{\perp} - dq_{\perp\to\parallel} - de_{w,\perp}$$

(Transfer heat)

Self generated waves caused by plasma anisotropy

$$du_{\parallel} = dw_{\parallel} + dq_{\perp\to\parallel} - de_{w,\parallel}$$

The net change of internal energy per particle

$$du = dw - de_{w,tot}$$

The change in electron Entropy

- For a non relativistic bi-Maxwellian plasma with perpendicular temperature and parallel temperature

The entropy per particle

$$s \equiv -\frac{\int d^3p f \ln f}{\int d^3p f} = \ln\left(\frac{T_\perp T_\parallel^{1/2}}{n}\right) + C$$

f(p) phase space distribution

$$ds = \left[\frac{1}{2} d\ln\left(\frac{T_\parallel}{\left(n/B\right)^2}\right)\right] \cdot \left[1 - \frac{T_\parallel}{T_\perp}\right] - \frac{de_{wtot}}{T_\perp},$$

Entropy of the gas can be changed
- by heat transfer between par. & per. C.
- or via wave energy

$$ds = -\left[d\ln\left(\frac{T_\perp}{B}\right)\right] \cdot \left[\frac{T_\perp}{T_\parallel} - 1\right] - \frac{de_{wtot}}{T_\parallel}.$$

1. A temperature anisotropy
2. Mechanism to break the adiabatic invariance

Shock structure

- Reference Run

$$M_{s,0} = \frac{V_0}{c_s} = \frac{V_0}{\sqrt{2\Gamma k_B T_0 / m_i}} = 3, \qquad \frac{m_i}{m_e} = 16$$

$$M_s = \frac{V_1}{c_s}, \qquad M_s = M_{s,0}\left(1 + \frac{1}{r(M_s) - 1}\right),$$

$$r(M_s) = \frac{\Gamma + 1}{\Gamma - 1 + 2/M_s^2}.$$

$$\beta_{p0} = \frac{8\pi n_0 k_B \left(T_{i0} + T_{e0}\right)}{B_0^2} = 16$$

- 2 main locations are identified where the electron entropy increases: the shock ramp and the site where proton-driven waves grow

Proton dynamics and proton-driven Instabilities

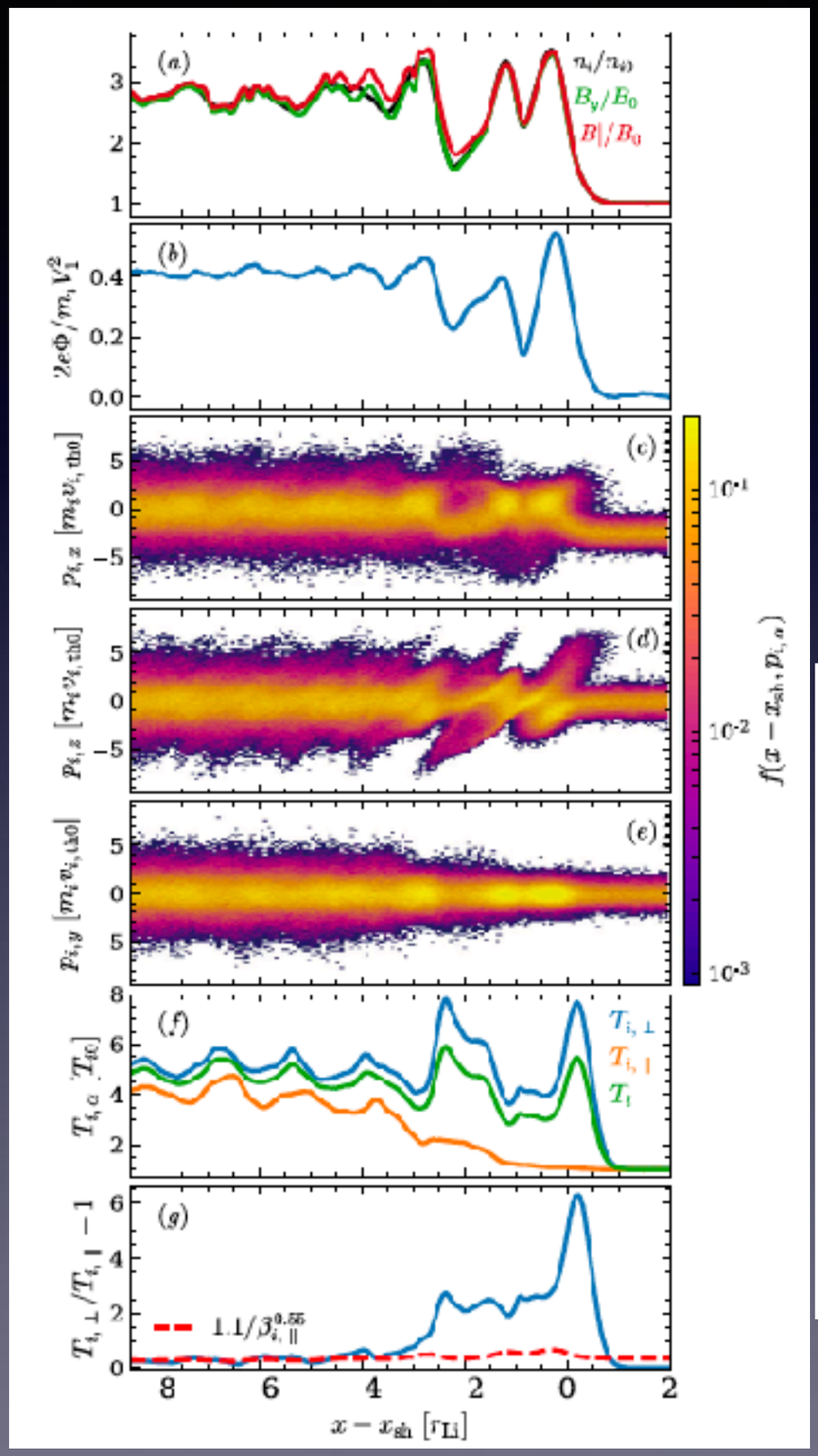

- Density Oscillations are on larmor length scale after the over-shoot and relaxes to 2.8.
- Density compression at the shock reaches to 3.5 over a distance
- The density pileup at the shock is related to the electrostatic potential near shock transition region
- Reaches up to 60% of the incoming proton energy. Significant fraction of protons are reflected. That leads to pile up in front of the shock.
- The amplitude of the density oscillations gets smaller as the gyrating reflected protons become more and more phase mixed with the directly transmitted protons.
- The decrease in the perpendicular temperature and the resulting increase in parallel temperature suggests that protons are being scattered in the pitch angle.
- Oscillations gets smaller as the gyrating reflected protons become more and more phase-mixed with the directly transmitted protons.

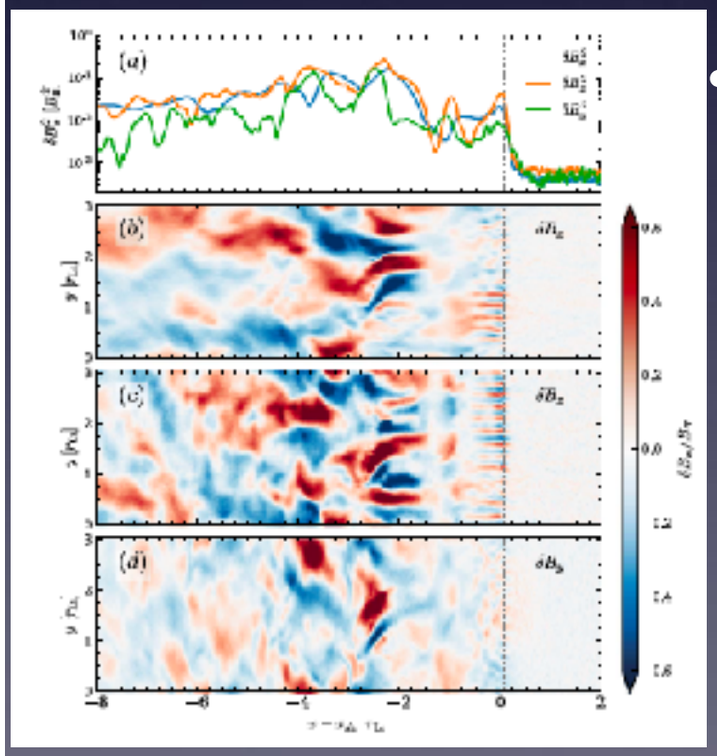

- Dominant modes (in x,z), ky
  Consistent with Pro. CI
- Weaker mode (oblique wave vector)
  Mirror mode
- PCI & MI sourced by PTA
  - PA provides free energy for the growth.

FIG. 1 Shock structure and Proton dynamics
FIG. 2 1D and 2D structures of magnetic fluctuations

Electron dynamics and heating

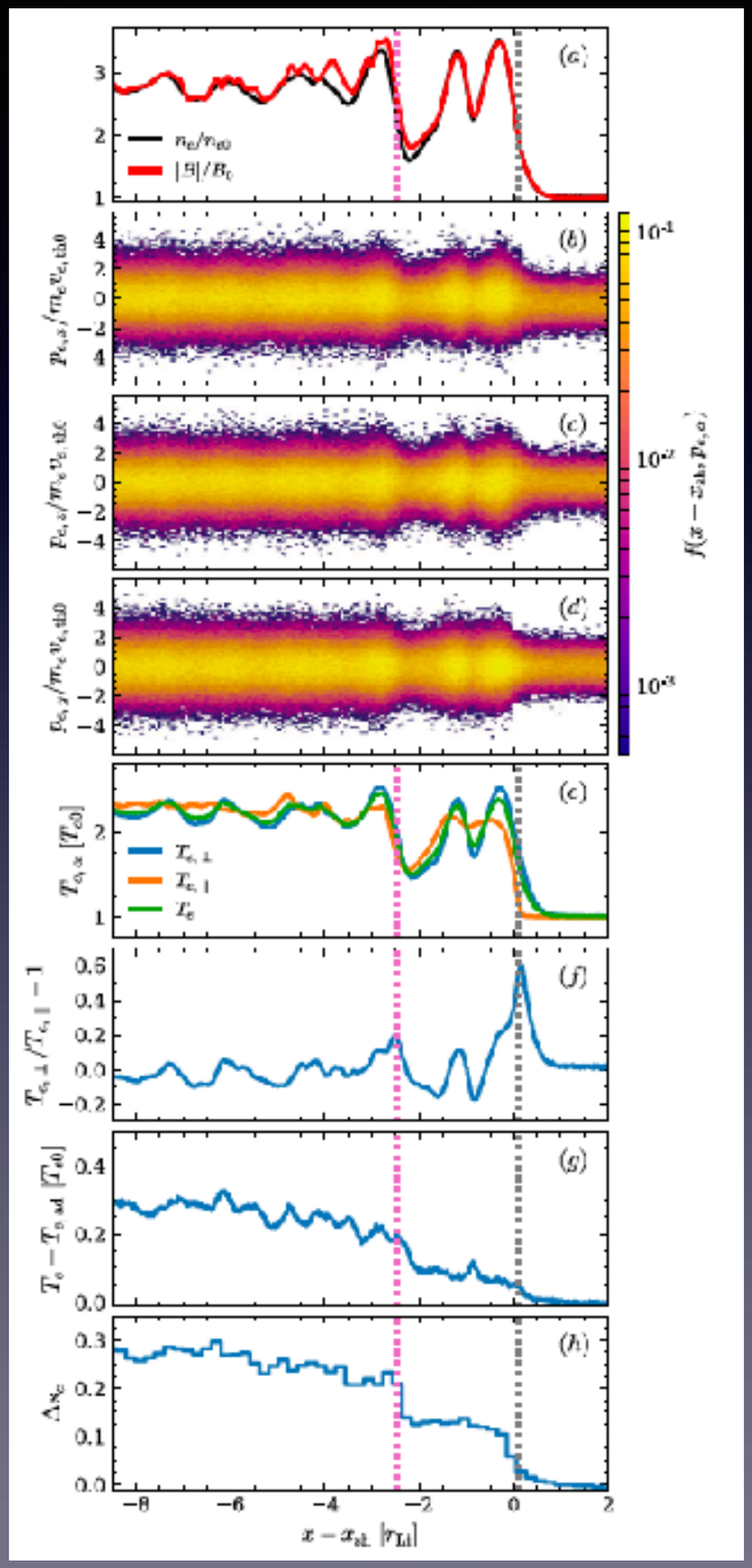

- Due to their opposite charge and much smaller Larmor radius, the dynamics of electrons is drastically different.
- Resembles with the protons; ensures charge neutrality.
- Small degree of charge separation at the shock is must for ϕ (far downstream seems OK)
- Electrons have opposite charge than protons, they are not reflected back upstream by ϕ. Hence no population unlike protons ahead of the shock.
- Profile of perpendicular temperature follows closely density compression (start to rise in front of the shock)
- The increase in perpendicular temperature at the shock gives strong electron anisotropy. EWI is excited. Creates small wavelength transverse magnetic waves.
- EWI provides a mechanism for electron pitch angle scattering, thus reduces TA.
- $T_\perp$ is dominant. However, $T_\parallel$ is not constant across the shock requires non adiabatic processes.
- The excess electron temperature T_e (mean temperature) over the adiabatic expectation.

Adiabatic prediction $$\frac{T_{e,ad}}{T_{e0}} = \left(\frac{n_e}{n_{e0}}\right)^{2/3}$$

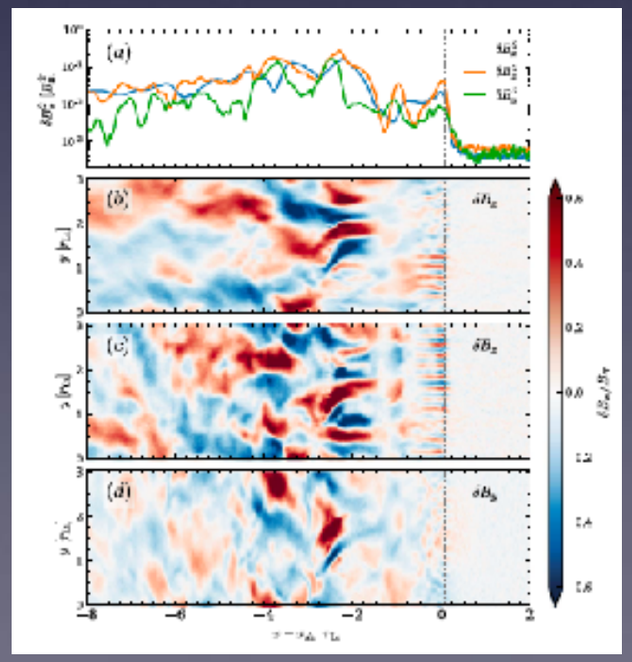

FIG. 3 Shock structure and electron dynamics

Power Spectra

$x - x_{sh} \simeq 4c/w_{pe}$

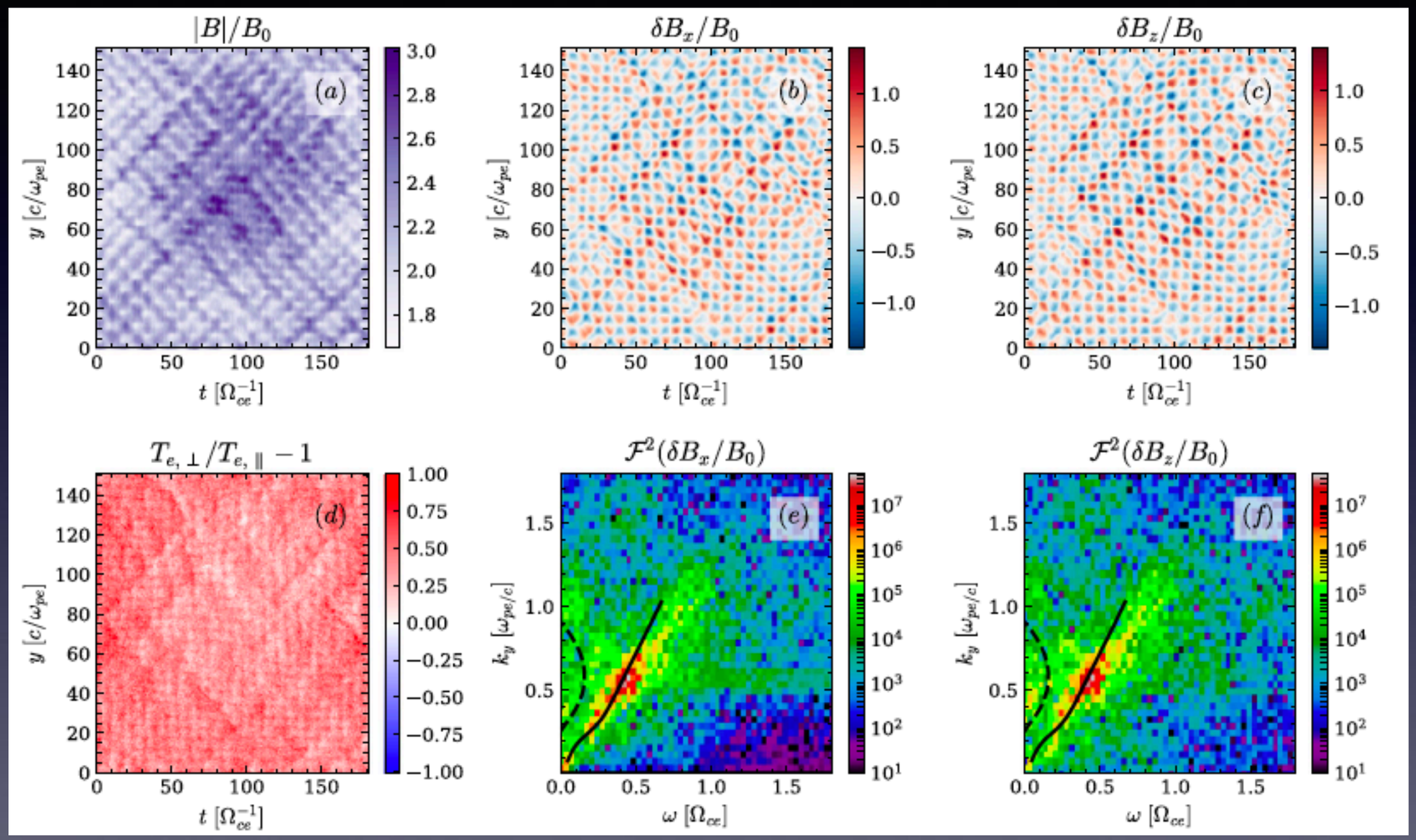

- The resulting theoretical prediction (EWI) for the real part of the frequency is shown with a black solid line panels in (e) and (f) and it matches extremely well the contours of the power spectrum.
- The imaginary part of the frequency (growth rate) is plotted with a dashed black curve (the value of Ky giving fastest growth matches well).

Anisotropy driven long wavelength proton modes $x - x_{sh} \simeq -2.5 r_{Li} \simeq -122\, c/w_{pe}$

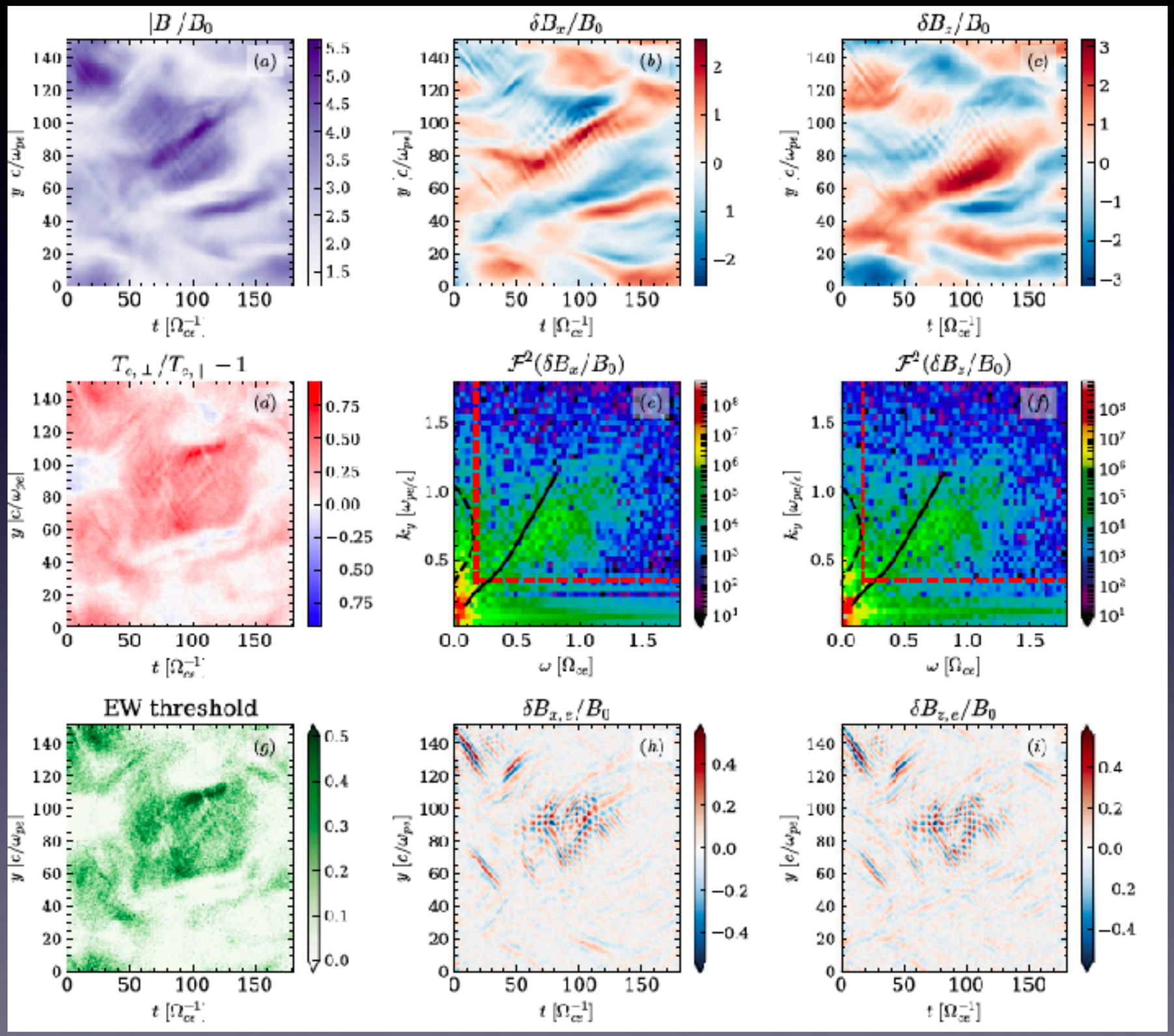

Electron heating in the shock ramp

- Large-scale compression is included in PIC.
- The first increase in electron entropy happens in the shock ramp.
- Electrons becomes anisotropic and they trigger whistler waves.
- Both electrons and protons will develop TA, means development of electrons and protons anisotropy driven modes

By electron whistler Instability

- Case 1: (out of plane) $B_0 \parallel \hat{z}$
- Case 2: (in plane) $B_0 \parallel \hat{y}$
- Simulation Box direction $\hat{y}$
- Growth of EWI is artificially suppressed
- Follow adiabatic heating
- No transfer of heat from perpendicular to parallel
- Electron entropy remains constant.

Application to the Reference Shock

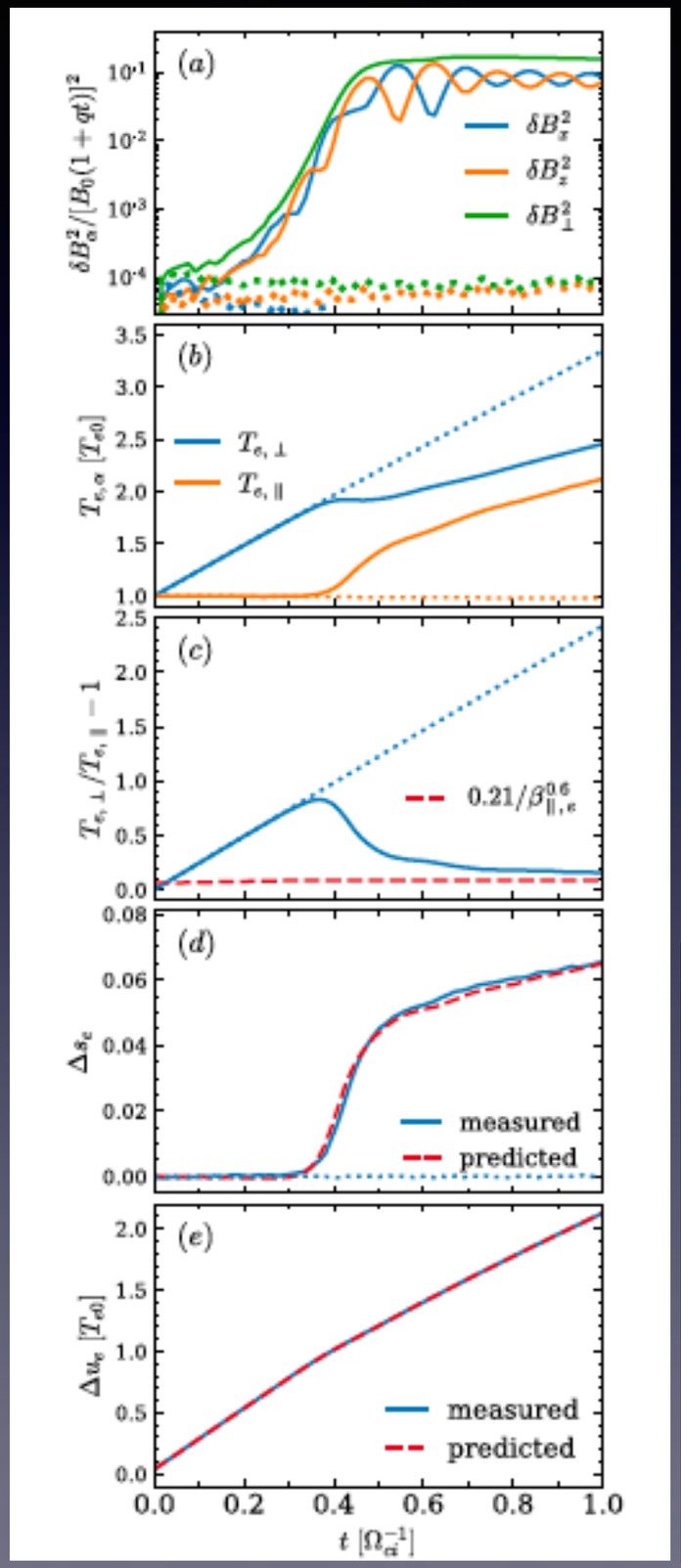

Figure 7. Time evolution of various space-averaged quantities in a 1D periodic box whose compression rate $q = 2.5\,\Omega_{ci}$ is chosen to mimic the effect of the shock ramp. We compare two field geometries, with the background field lying either along the y axis of the simulation box ("in-plane" configuration, solid lines) or along the z direction perpendicular to the box ("out-of-plane" configuration, dotted lines): (a) energy in magnetic field fluctuations, normalized to the energy of the compressed magnetic field (the legend is appropriate for the in-plane configuration, whereas for the out-of-plane case the orange line refers to δB_y^2); (b) electron temperature perpendicular ($T_{e,\perp}$, blue lines) and parallel ($T_{e,\parallel}$, orange lines) to the background field; (c) electron temperature anisotropy (blue lines), and comparison with the threshold of the electron whistler instability, as in Equation (29) (dashed red line); (d) electron entropy change, measured from the electron distribution function as in Equation (26) (blue solid) or predicted from Equation (33) (red dashed); (e) electron energy increase in units of $k_B T_{e0}$, measured directly (blue solid) or predicted using Equation (32) (red dashed).

Dependence on mass ratio

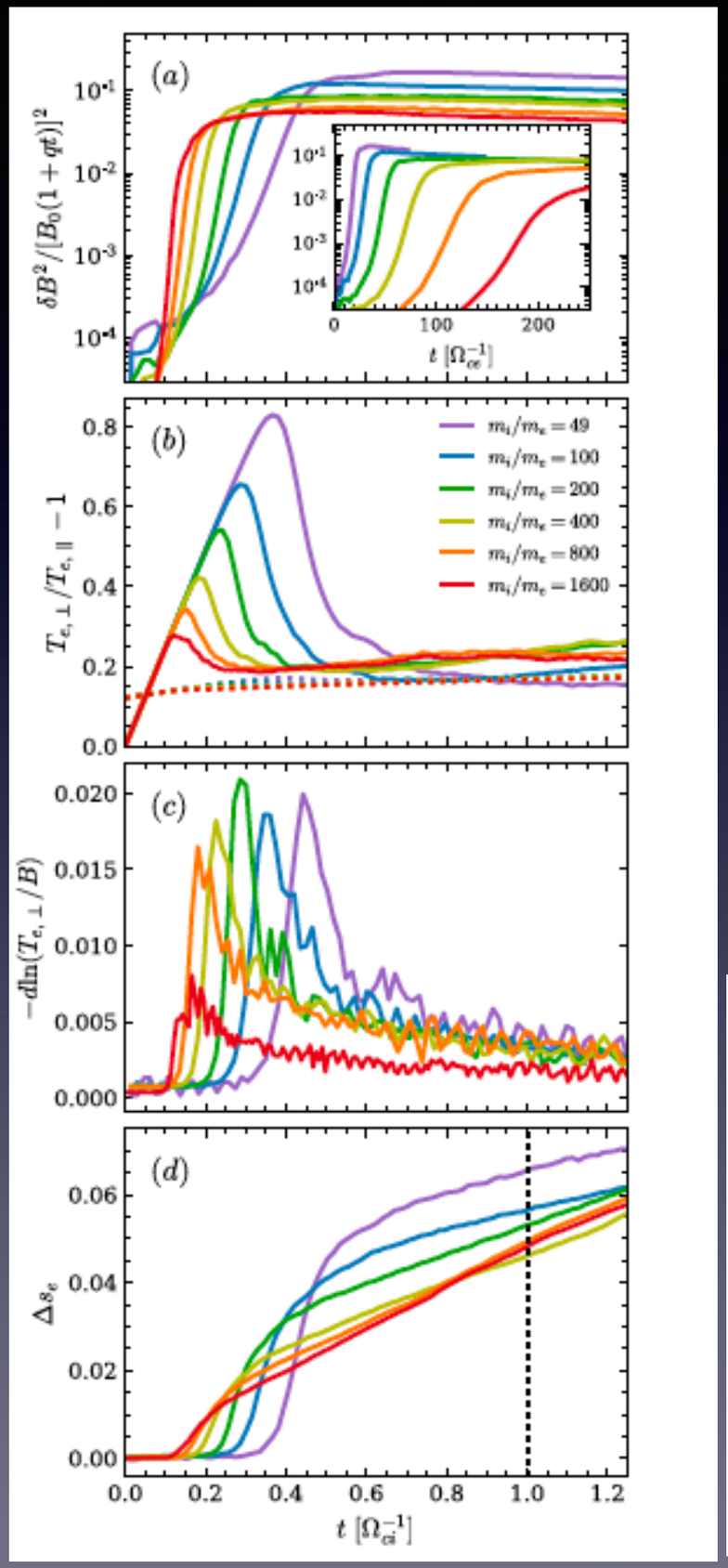

- Whistler waves are sufficiently strong to disrupt the adiabatic invariance

Figure 8. Dependence on mass ratio (up to $m_i/m_e = 1600$) of various space-averaged quantities in a 1D periodic box with compression rate $q = 2.5\ \Omega_{ci}$ (the legend is in panel (b)). The background field is aligned with the box (in-plane configuration). We plot (a) energy in magnetic field fluctuations, normalized to the energy of the compressed field; (b) electron temperature anisotropy (solid lines) and threshold condition for the electron whistler instability (dotted lines with the same color coding as the solid lines); (c) rate of violation of adiabatic invariance $-d\ln(T_{e,\perp}/B)$; (d) electron entropy change, measured from the electron distribution function as in Equation (26). After $\Omega_{ci}t \sim 1$ (vertical dotted black line in panel (d)), which corresponds to the end of the compression phase in the shock ramp, the entropy change is nearly independent of the mass ratio.

Thank you